Applied Numerical Modeling in Geomechanics – 2020 – Billaux, Hazzard, Nelson & Schöpfer (eds.) Paper: 11-04

Using rigid block / *FLAC3D* coupling in mine-scale simulations

Matthew D. Purvance & Tryana Garza-Cruz
Itasca Consulting Group, Inc., Minneapolis, MN, USA

1 INTRODUCTION

Underground excavations in deep, brittle, highly stressed environments present numerous engineering challenges. For instance, tunnel instabilities in the form of stress localizations (i.e., fracturing, spalling and/or bulking) may result in catastrophic consequences. Continuum models effectively capture large-scale, emergent material response to mining stresses but often cannot explicitly model localizations. Instead, the effects of localizations are modeled via constitutive models. Discrete element (DEM) models, alternatively, can explicitly model localizations along with emergent material response but require significantly more computational effort. Combining continuum and discrete approaches offers significant promise, allowing for explicit localizations in regions of interest along with efficient modeling of large-scale material response outside these regions. This work demonstrates such coupling via a generic block/panel cave mining scenario at depth using wall-zone coupling in *PFC 6* (Itasca 2018). *FLAC3D* zone faces are wrapped with *PFC* walls; as contact forces arise between discrete objects and the wall facets, equivalent force systems are computed and applied to the zone faces. Meanwhile, the facet velocities/positions are slaved to the corresponding gridpoints.

Pierce et al. (2007) used *PFC* with spherical particles to simulate brittle rock masses via the Synthetic Rock Mass (SRM) approach, inserting smooth-joint contacts aligned with fractures to provide planar failure surfaces inside a bonded particle specimen. Although SRM models can be used to effectively gain insights into rock mass behavior, they suffer from significant porosity (due to the spherical particle packing), long computational times for large models, and from the small-strain nature of the smooth-joint contact logic. Thus, those models cannot effectively reproduce the fragmentation/bulking behavior observed in real rock masses under large strains. Garza-Cruz et al. (2014) used *3DEC* to investigate tunnel excavations exposed to approximate mining stresses. Using zoned blocks that are joined away from the tunnel, that work effectively coupled continuum and discrete models, representing the discrete rock mass via a zero-porosity packing of deformable blocks. As joint failure occurs, blocks naturally rotate to produce bulking near the tunnel surface with discrete fragment formation indicating regions of failure.

In this work, a generic block/panel cave mining geometry at depth is simulated where the discrete region is modeled with *PFC* rigid blocks (hereafter termed rblocks). Not only does this allow for significant computational speed improvements over similar *3DEC* models (~2.5-3.5 times faster model runs), the rblocks also overcome the deficits inherent in the SRM approach. A calibrated rblock model is created, walls are slaved to zone faces, and in situ stresses are installed. Production drifts are excavated and a 0.1 MPa support pressure is applied. A bulking algorithm is applied to zones to simulate orebody undercutting and mobilization due to caving while the effects on the discrete region are monitored. The results demonstrate the ability of this methodology to simulate large-scale scenarios with localization.

2 DESIGN AND ANALYSIS

In this generic block/panel caving model at depth, production drifts are driven below drawbells and stub production drifts are driven below the drawpoints at an angle of 30 degrees to the production drifts. The material in the drawbells is modeled via zones while a section intersecting the central production drift between drawbells is modeled via rblocks (Fig. 1a). The entire volume has been meshed with tetrahedra, grading to smaller tetrahedra in the extraction level. In the discrete region, the tetrahedra grade further from ~3.5 m edge lengths down to ~0.035 m edge lengths. The tetrahedra do not conform to the drift geometries as meshing to a surface geometry can introduce artificial arches leading to an overprediction of stability. Instead rblocks are cut by the drifts to mitigate this issue. The extraction level is modeled at 900 m depth by applying a stress boundary condition at the top of the model consistent with the overburden. The horizontal stresses in the direction of the production drifts and perpendicular to these drifts are 2 and 1 times the vertical stress, respectively. The contact forces in the discrete region are assigned by computing tractions consistent with the stress tensor at the contact positions. The Young's modulus of the zones is 14 GPa with Poisson ratio 0.25. The cavehoek constitutive model without ubiquitous joints is used in the zones, giving the zones 42.5 MPa UCS strength.

The target UCS and tensile strengths of the discrete regions are 42.5 MPa and 4.25 MPa, respectively, consistent with the zone emergent strength. A cylindrical specimen of rblocks has been carved from the center of the discrete region for calibration. Note that unlike for spherical DEM models, both the target Poisson ratio and UCS/tensile ratio are easily achieved with rblocks. The rblocks are scaled to ensure overlap and eroded to cull vertex-vertex and edge-edge contacts. The vertex-vertex and edge-edge contacts are inhibited, greatly improving computational performance without impacting model response. Every 100 cycles the inhibited contacts are checked for reactivation. The contact areas are computed based on the rblock-rblock or rblock-facet overlaps. The softbond contact model, without softening or rolling resistance, has been used with non-default parameters given in Table 1. A normal distribution of tensile strengths has been specified with cohesive strengths 2.5 times the tensile strengths. After stress initialization and equilibration, rblocks and zones in the production drifts have been removed and equivalent support pressures applied to the drift faces to allow for consistent stress relaxation throughout the model. The resulting model consists of ~261,000 rblocks, ~2,900 wall facets, ~528,000 active contacts, ~8,700,000 inhibited contacts, and ~656,000 zones.

Excavation of the production drifts proceeds by relaxing the support pressures in 0.5% increments, equilibrating the model to an average ratio of 1e-5 between each step. The displacements and stresses after complete relaxation are shown in Figures 1b through 1d. The continuity in displacements and stresses demonstrates that the discrete material has been calibrated appropriately and that the coupling effectively transfers forces from the discrete region to the continuum. Few contact bonds have broken in response to the support pressure relaxation, and no fragments exist. Fragments are defined as groups of rblocks that are bonded with one another but not to any other rblock fragments. Once the 0.1 MPa support pressure has been applied to the drift walls production commences.

Table 1. RBlock material characteristics with corresponding softbond contact model property/method names and values. Properties not specified remain at the default values.

Young's modulus	14 GPa (set via the deformability contact method using emod = 51.6 GPa and kratio = 3.6)
Poisson ratio	0.25 (set via the deformability contact method using emod = 51.6 GPa and kratio = 3.6)
Friction coefficient (residual friction)	fric = 0.6
Incremental normal force computation	sb_bmode = 1
Inhibit rolling resistance contribution after bond breakage	sb_bmul = 0
Bond tensile strength	sb_ten drawn from a normal distribution with mean 16.3 MPa and standard deviation 8.15 MPa
Bond cohesive strength	sb_ten drawn from a normal distribution with mean 40.7 MPa and standard deviation 20.4 MPa
Bond friction angle	sb_fa = 30 degrees

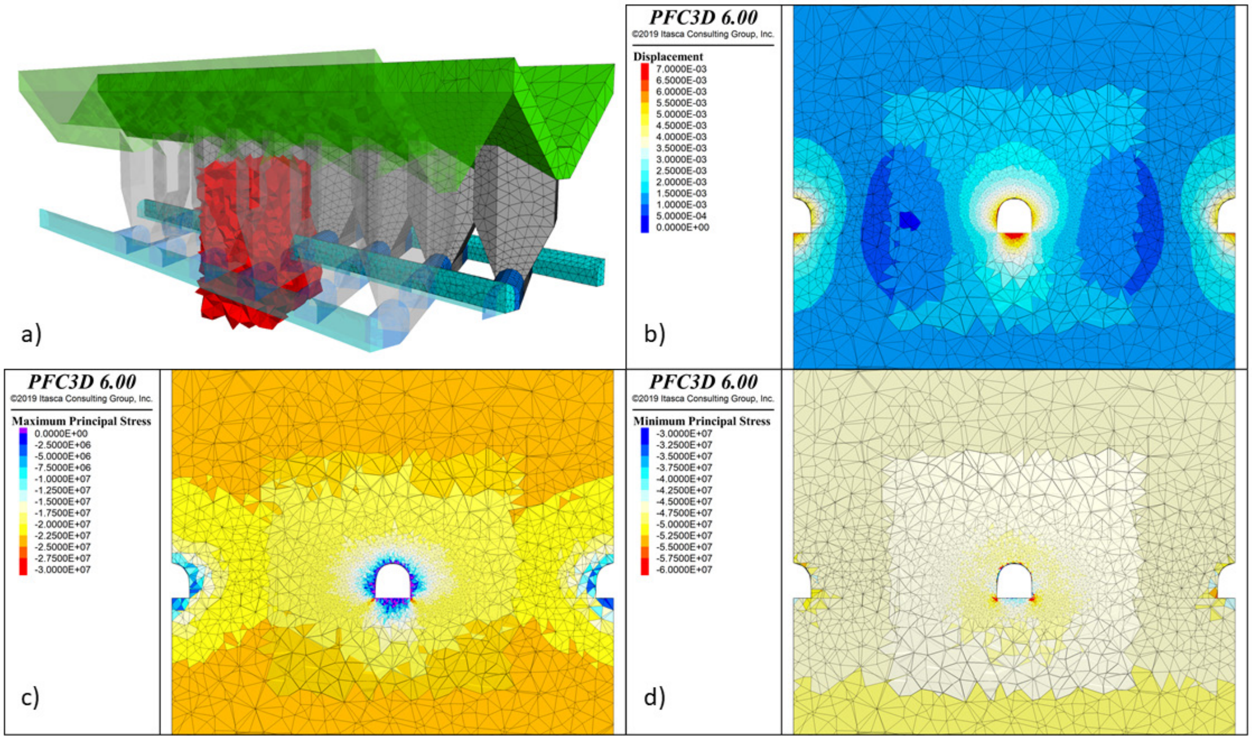

Figure 1. a) Generic block/panel caving model geometry at depth with drawbells (gray), production drifts (cyan), stub production drifts (blue), rblocks (red), and undercut regions (green). Zone and rblock displacements (b), maximum principal stresses (c), and minimum principal stresses (d) after production drift relaxation. All plots depict values on a cut plane through the center of the discrete region that is perpendicular to the production drift. This orientation is different from Figure 2 below. Due to rendering and contour computation differences, colors used in the contours may not render exactly between rblocks and zones. The rblock region is central in all plots.

3 RESULTS AND DISCUSSION

To initiate caving, the orebody is undercut (green region in Fig. 1a). A bulking algorithm is applied to zones to simulate this process, consisting of incrementally reducing stresses in scheduled zones, along with modifying the cavehoek model properties to simulate an increase in porosity to 30%. The bulking algorithm is also applied to drawbells sequentially, with stub production drifts excavated directly beneath the center of the bulked drawbells (Fig. 1a). Production progresses from the front of the model and propagates toward the discrete region. Mobilization of the orebody for extraction is also simulated via the bulking algorithm. Zones within ellipsoidal Isolated Movement Zones (IMZ's) (Pierce 2010) are identified above drawpoints based on a tonnage schedule, and the porosity is reduced in these zones accordingly.

In Figures 2a and 2b, undercutting extends beyond the discrete region and IMZs exist above the first 2 drawbells. Approximately 3,000 fragments have developed, extending up to ~1 m from the drift roof and side walls. Fragments roughly correspond with purple regions in the remaining figures. Notice that at this stage of the excavation few fragments exist below the drift floor. The maximum principal stresses in the extraction level have lowered by roughly a factor of 2 (from ~ 20 MPa to ~ 10 MPa) while the minimum principal stresses have lowered by about 20% compared with the stresses after production drift excavation. In Figures 2c and 2d, the drawbells next to the discrete region have been bulked and the stub drift has been excavated/supported in the discrete region. In order to simulate the response of rblocks within drawbells, contact stresses within the drawbell regions have been assigned forces corresponding to adjacent zone stresses. In addition, these contacts have not been allowed to break. These actions are required so that stresses within the drawbell rblock regions remain consistent with the stresses within adjacent drawbell zone regions.

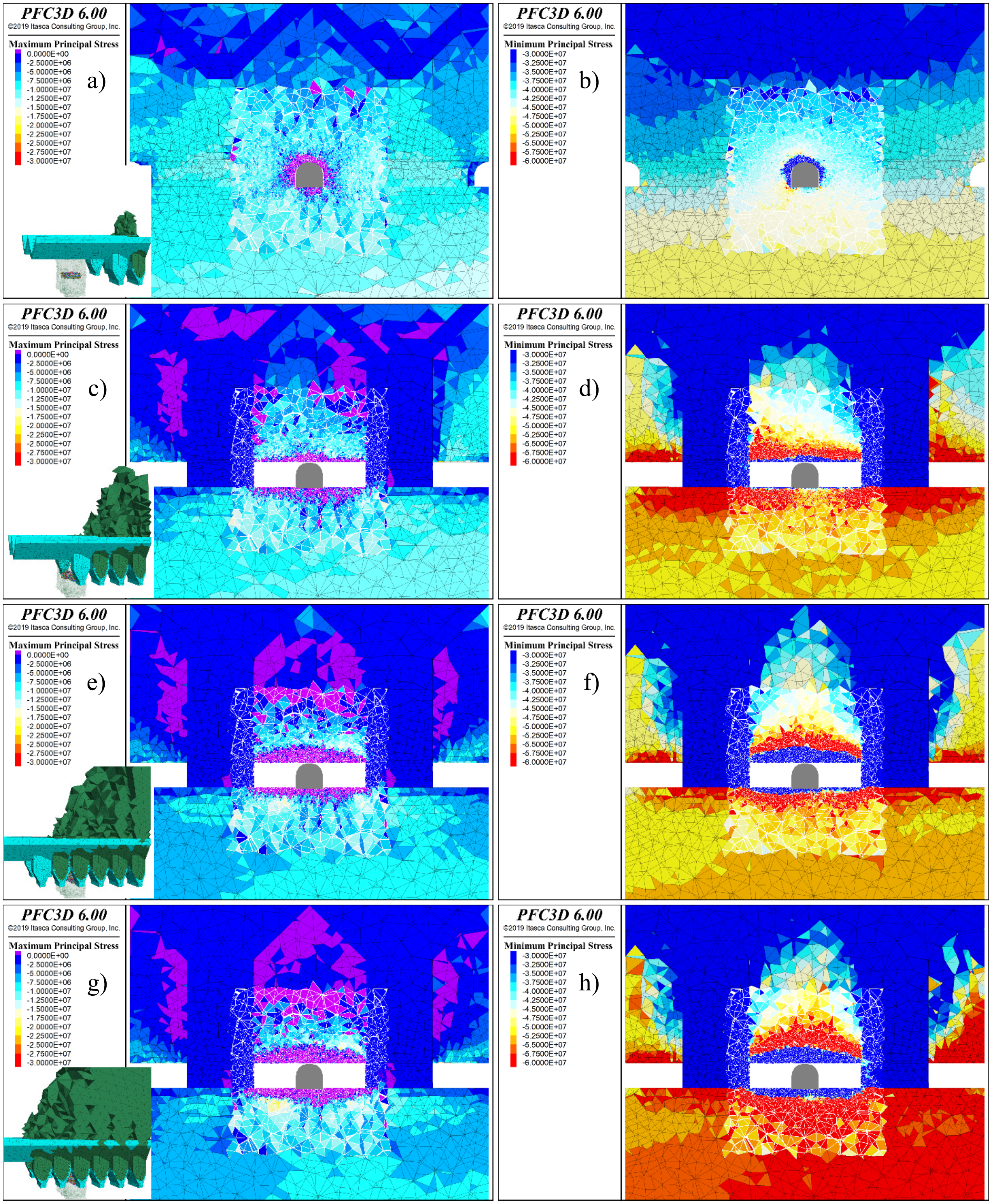

Figure 2. Insets show the bulked (cyan) and produced (green) regions. Gray regions are the production drift silhouettes. Left plots (a, c, e, and g) show the maximum principal stress, while right plots (b, d, f, and h) show the minimum principal stress at different stages of production. All plots depict values on a cut plane through the center of the discrete region aligned with the stub production drift. This orientation is different from Figure 1. Note that due to rendering and contour computation differences, colors used in the contours may not render exactly between rblocks and zones. The rblock region is central in all plots.

There are ~5,500 fragments at this stage of the simulation, with added fragmentation primarily located around the exterior of the stub production drift. The extent of fragmentation into the production drift roof/floor has not changed substantially, though more tensile regions exist below the production drift. Figures 2e and 2f show the stress state after two additional drawbells have been bulked with production extending beyond the discrete region. The number of fragments has nearly doubled to ~11,000, roughly doubling the volume of fragmented rock. Fragments extend above the production drift to ~2 m as the stress is eroded above the extraction level. Fragmentation has also developed below the drift, extending to ~0.5 m. The fragmentation extends the farthest in the region where the production and stub production drifts intersect, directly above/below the production drift. Figures 2g and 2h illustrate a later stage of production, with ~13,000 fragments extending to ~2.5 m above and ~1 m below the production drift.

4 CONCLUSIONS

The introduction of coupling between discrete and continuum methods in *PFC*, along with the advent of rblocks, allows for *PFC* to effectively model large-scale scenarios of intact rock with explicit localization. This work demonstrates the impact of generic block/panel cave mining stresses on production drift stability at depth. The *PFC* model is substantially faster (~2.5-3.5 times faster model runs) than similar *3DEC* models. Continuity of displacements and stresses during drift relaxation demonstrates the efficacy of the coupling. Continued production has significant impact on the drift stability as seen through the principal stresses and fragmentation development during varying stages of production. Though a simple support pressure has been applied to the drift faces, structural elements could be used in the discrete region to explicitly model the support member responses.

REFERENCES

Garza-Cruz, T.V., Pierce, M.E. & Kaiser, P.K. 2014. Use of 3DEC to study spalling and deformation associated with tunneling at depth. In M. Hudyma & Y. Potvin (eds.), *Proc. of the Seventh Intern. Conf. on Deep and High Stress Mining*, *Perth*, *16-18 September 2014*. Nedlands: Australian Centre for Geomechanics.

Itasca Consulting Group, Inc. 2018. *PFC – Particle Flow Code, Version 6.0 Software Documentation*. Minneapolis: Itasca.

Pierce, M.E. 2010. *A Model for Gravity Flow of Fragmented Rock in Block Caving Mines*. Sustainable Minerals Institute: University of Queensland.

Pierce, M.E., Mas Ivars, D., Potyondy, D. & Cundall, P.A. 2007. A synthetic rock mass model for jointed rock. In Eberhardt, Stead & Morrison (eds.), *Proc. 1st Canada-US Rock Mech. Symp., Vancouver, 27-31 May 2007*. London: Taylor & Francis Group.